

**MICROEXPLOSIONS AND IGNITION DYNAMICS IN
ENGINEERED ALUMINUM/POLYMER FUEL PARTICLES**

by

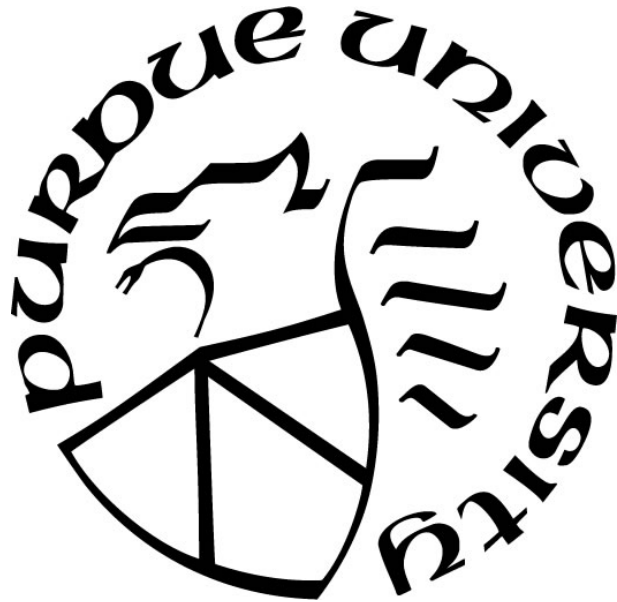
Mario A. Rubio

A Thesis

Submitted to the Faculty of Purdue University

In Partial Fulfillment of the Requirements for the degree of

Master of Science in Mechanical Engineering



Department of Mechanical Engineering

West Lafayette, Indiana

May 2017

ProQuest Number: 10268368

All rights reserved

INFORMATION TO ALL USERS

The quality of this reproduction is dependent upon the quality of the copy submitted.

In the unlikely event that the author did not send a complete manuscript and there are missing pages, these will be noted. Also, if material had to be removed, a note will indicate the deletion.



ProQuest 10268368

Published by ProQuest LLC (2017). Copyright of the Dissertation is held by the Author.

All rights reserved.

This work is protected against unauthorized copying under Title 17, United States Code
Microform Edition © ProQuest LLC.

ProQuest LLC.
789 East Eisenhower Parkway
P.O. Box 1346
Ann Arbor, MI 48106 – 1346

THE PURDUE UNIVERSITY GRADUATE SCHOOL
STATEMENT OF THESIS APPROVAL

Dr. Steven F. Son, Chair

Department of Mechanical Engineering

Dr. Lori J. Groven

Department of Mechanical Engineering

Dr. Ibrahim E. Gunduz

Department of Mechanical Engineering

Approved by:

Dr. Jay P. Gore

Head of the Departmental Graduate Program

The work that I have completed and more importantly the knowledge, experiences and personal insight I gained from pursuing my master's degree here at Purdue University, I dedicate to my family.

ACKNOWLEDGMENTS

I must acknowledge many people for their support and guidance throughout this work. My primary advisor Professor Steven Son and faculty members Dr. Lori Groven and Dr. Emre Gunduz, whose invaluable expertise in the field of energetics and most of all patience, allowed me to complete the work presented here. Dr. Travis Sippel introduced me to the topic of mechanical activation of composite fuel particles and provided invaluable expertise in the subject matter. Additionally Dr. Sippel provided mentorship and friendship instrumental to the completion of this work.

To all the staff, faculty and especially fellow graduate research students who helped in countless ways both academically and professionally. They inspired and challenged me to conduct high quality research in the tradition of Maurice J. Zucrow Laboratory. Very special thanks and appreciation must be extended to Ph.D. Candidates David E. Kittel and Jesus Mares. If not for their help and support academically I would not have been able to complete my program. Their time, patience and most importantly friendship is very much appreciated.

I am also indebted to the National GEM Consortium MS Fellowship program and Delphi Thermal Systems. Their sponsorship and financial support for tuition and research fellowship stipends as well as summer internship stipends allowed me to pursue my and attain my degree.

TABLE OF CONTENTS

LIST OF FIGURES	vii
LIST OF TABLES	viii
LIST OF ABBREVIATIONS.....	ix
ABSTRACT.....	x
1. INTRODUCTION	1
1.1 Introduction.....	1
1.2 Research Objectives.....	3
2. BACKGROUND AND MOTIVATION.....	4
2.1 Agglomeration and Two-Phase Flow Losses	4
2.2 Mechanical Activation.....	5
2.3 Materials Selection.....	7
2.3.1 Polytetrafluorethylene Inclusion Material.....	7
2.3.2 Low Density Polyethylene Inclusion Material	8
3. MATERIALS PREPARATION AND EXPERIMENTAL APPARRATUS.....	9
3.1 Materials Preparation and Milling	9
3.2 Morphology and Microstructural Characterization of Al/PTFE and Al/LDPE.....	10
3.3 Single Particle Ignition Experiments	11
3.4 Product Size Distributions	14
4. RESULTS AND DISCUSSION.....	15
4.1 Al/PTFE 70/30 wt.% (20, 60 min MA)	15
4.2 Al/PTFE 90/10 wt.% (60 min MA)	21
4.3 Al/LDPE 90/10 wt.% (52 hr MA).....	24
5. CONCLUSIONS	28
LIST OF REFERENCES	30
APPENDIX A. DATA TABLES OF RESULTS FROM IGNITION EXPERIMENT....	33
Results from laser ignition experiments for 70/30 Al/PTFE 20 min MA.....	33

Continued.....	34
Results from laser ignition experiments for 70/30 Al/PTFE 60 min MA.....	35
Results from laser ignition experiments for 90/10 Al/PTFE 60 min MA.....	36
Results from laser ignition experiments for 90/10 Al/LDPE 52 hr MA.....	37

LIST OF FIGURES

Figure 2.1. Spex Mill 8000 vibratory shaker mill.....	6
Figure 2.2. U.S. Stoneware roller mill.....	6
Figure 3.1. Representative secondary signal image of an Al-LDPE particle.	11
Figure 3.2. Schematic of the experimental apparatus	13
Figure 4.1. Image sequences captured from laser ignition of 70/30 wt.%	16
Figure 4.2. Product particle size distributions for 70/30 wt.% Al/PTFE	17
Figure 4.3. Initial particle size effect on microexplosion of composite fuel	18
Figure 4.4. Ignition delays of 70/30 wt.% Al/PTFE milled for 20 and 60 min MA	20
Figure 4.5. Image sequences of the reaction dynamics of 90/10 wt.%	22
Figure 4.6. Ignition delay of 90/10 wt.% Al/PTFE (60 min MA).	23
Figure 4.7. Product particle size distribution.	24
Figure 4.8. Image sequences capturing reaction dynamics.....	26
Figure 4.9. Ignition delay of 90/10 wt.% Al/LDPE.....	27
Figure 4.10. Product particle size distribution of 90/10 wt.% Al/LDPE 52hr.....	28

LIST OF TABLES

Table 3.1. Heating flux and camera settings for ignition experiments.....	13
Table A.1. Results from laser ignition experiments for 70/30 Al/PTFE 20 min MA.....	33
Table A.2. Results from laser ignition experiments for 70/30 Al/PTFE 60 min MA.....	35
Table A.3. Results from laser ignition experiments for 90/10 Al/PTFE 60 min MA.....	36
Table A.4. Results from laser ignition experiments for 90/10 Al/LDPE 52 hr MA.....	37

LIST OF ABBREVIATIONS

ABBREVIATION	DESCRIPTION
AP	Ammonium Perchlorate
ARM	Arrested Reactive Milling
MA	Mechanical Activation
LDPE	Low Density Polyethylene
PTFE	Polytetrafluoroethylene
20 min MA	20 minute high energy Mechanically Activated
60 min MA	60 minute high energy Mechanically Activated
52 hr MA	532 hour low energy Mechanically Activated

ABSTRACT

Author: Rubio, Mario, A. MSME

Institution: Purdue University

Degree Received: May 2017

Title: Microexplosions and Ignition Dynamics in Engineered Aluminum/Polymer Fuel Particles.

Major Professor: Steven Son.

Aluminum particles are widely used as a metal fuel in solid propellants. However, poor combustion efficiencies and two-phase flow losses result due in part to particle agglomeration. Recently, engineered composite particles of aluminum (Al) with inclusions of polytetrafluoroethylene (PTFE) or low-density polyethylene (LDPE) have been shown to improve ignition and yield smaller agglomerates in solid propellants. Reductions in agglomeration were attributed to internal pressurization and fragmentation (microexplosions) of the composite particles at the propellant surface.

Here, we explore the mechanisms responsible for microexplosions in order to better understand the combustion characteristics of composite fuel particles. Single composite particles of Al/PTFE and Al/LDPE with diameters between 100-1200 μm are ignited on a substrate to mimic a burning propellant surface in a controlled environment using a CO_2 laser in the irradiance range of 78-7700 W/cm^2 . The effects of particle size, milling time, and inclusion content on the resulting ignition delay, product particle size distributions, and microexplosion tendencies are reported. For example, particles with higher PTFE content (30 wt.%) had laser flux ignition thresholds as low as 77 W/cm^2 , exhibiting more burning particle dispersion due to microexplosions compared to the other materials considered. Composite Al/LDPE particles exhibit relatively high ignition thresholds compared to Al/PTFE particles, and microexplosions were observed only with laser fluxes above 5500 W/cm^2 due to low LDPE reactivity with Al resulting in negligible

particle self-heating. However, results show that microexplosions can occur for Al containing both low and high reactivity inclusions (LDPE and PTFE, respectively) and that polymer inclusions can be used to tailor the ignition threshold. This class of modified metal particles shows significant promise for application in many different energetic materials that use metal fuel.

1. INTRODUCTION

1.1 Introduction

Development of engineered composite metallic fuels that have enhanced ignition and combustion characteristics is of critical need to improve propulsion systems performance. Aluminum (Al) is a widely used metallic fuel in propellants primarily because of its high gravimetric and volumetric oxidation enthalpy [1-3]. The addition of microscale Al fuel to high solids loading composite propellants has been shown to increase flame temperatures, burning regression rates and improve specific impulse (I_{sp}) rocket motors by up to 15% [4]. However microscale Al particles exhibit relatively slow combustion rates [2, 3] and long ignition delays, resulting in incomplete combustion and ignition failure in some cases. Additionally molten Al particles can coalesce on the propellant surface leading to the formation of agglomerates that can be orders of magnitude larger than the original fuel particles. Agglomerates that form at the surface are entrained into the rocket nozzle and exhaust flow contributing to two-phase flow losses in rocket motors [4,5]. In order to engineer composite fuel particles with tailored combustion characteristics that reduce ignition delay, increase Al combustion rate, and produce smaller agglomerates than conventional metal fuels, the ignition dynamics of engineered composite particles must be characterized.

Diffusion limited combustion inefficiency of microscale Al can be overcome by a reduction in average particle size. For example, replacing microscale aluminum with nAl in composite propellants has been shown to increase propellant burning rate [6], decrease Al particle ignition delay [7] and reduce agglomerate sizes in combustion products [8]. However; replacing microscale Al with nAl in composite propellant formulations can result in several unfavorable propellant properties and performance characteristics. The much higher relative oxide content (Al_2O_3) in nanoaluminum particles compared to microscale Al reduces the available combustion enthalpy resulting in lower propellant specific impulse [8]. The very high specific surface area ($\approx 10-50 \text{ m}^2/\text{g}$) of nAl particles causes the particles to agglomerate and form difficult to disperse aggregates during composite

propellant manufacture, resulting in high uncured propellant viscosity yielding propellants with poor mechanical strength [9-14]. Additionally, composite propellants prepared using nAl have been shown to suffer long term-degradation [15]. Although lower ignition thresholds in energetic materials can be achieved by using nanoscale aluminum, the much higher ignition sensitivity may negatively impact materials and operators during storage and handling. For example, nanoscale energetic materials are more prone to accidental ignition from electro-static discharge, impact and friction stimulus [16]. In addition to unfavorable propellant characteristics and increased safety risks there is also a much higher cost associated with nAl (\approx \$3000/kg) that is orders of magnitude more than microscale aluminum powder, inhibiting use of nAl in commercial propellants.

An alternative approach to enhance particle reactivity and reduce two-phase flow losses in rocket motors is to engineer composite fuel particles with tailored combustion characteristics through mechanical activation (MA). High-energy density reactive particles with ignition temperatures and ignition delays comparable to those of nAl can be produced with the proper selection of inclusion materials and milling parameters [2]. In recent studies investigating combustion of composite solid propellants, replacing neat Al with mechanically activated Al particles containing reactive (polytetrafluoroethylene, PTFE) or non-reactive (low-density polyethylene, LDPE) inclusion material has been shown to reduce ignition delays and metal particle ignition temperatures in propellant formulations [13, 14]. Additionally, observed decreases in particle agglomeration at the burning surface of propellants processed with PTFE or LDPE inclusion modified aluminum could potentially reduce two-phase flow losses in rocket motors [15, 16]. Reduced agglomerate formation results from fragmentation of the reacting composite particles due to microexplosions at the propellant surface.

During particle microexplosions, it is believed that intraparticle evolution of polymer decomposition gases and/or Al/PTFE reactions results internal particle pressurization, shattering the particles into much smaller fragments. Typically, ignition studies on MA composite fuel particles containing inclusion materials focus on bulk ignition properties of particles using a single set of parameters and the role of inclusion reactivity on

dynamics (e.g. microexplosions) is unclear [17]. The effects of milling energy and other particle parameters, such as initial particle size, stoichiometry, milling duration, and thermal environment on microexplosion tendency also remain unknown.

1.2 Research Objectives

The objectives of this research are two-fold: i.) Determine how initial particle size, milling duration, polymer inclusion type and polymer content affect ignition behavior and ii.) Develop an understanding of the role these parameters play in microexplosion tendency. To this end, ignition delay and product size distributions will be determined as functions of milling duration, initial particle size and varying inclusion materials at different laser heating fluxes. Combustion experiments with MA composite fuel particles are conducted on a substrate under various CO₂ laser fluxes that mimic the thermal environment at the surface of a burning propellant. The results will be used to determine microexplosion critical energy threshold for all materials as well as any particle size dependence of the parameters. If the ignition characteristics can be identified and the mechanisms for microexplosions are more clearly defined then mechanically activated composite fuel particles can be tailored for specific applications.

2. BACKGROUND AND MOTIVATION

2.1 Agglomeration and Two-Phase Flow Losses

The addition of aluminum fuel to composite propellants can improve rocket performance I_{sp} by as much as 15% by increasing propellant combustion temperatures and burn times [1-3]. However, disparities in the propellant surface burning temperatures (500-700 °C) and micro-scale aluminum particle ignition temperatures (1400-2200 °C) contribute to the formation of agglomerates at the propellant surface and result in two-phase flow losses [16].

As the flame front at the propellant surface combustion zone regresses, aluminum particles and aggregates are exposed. The exposed aluminum particles and aggregates with long residence times above aluminum melting temperatures (660-700 °C) can coalesce at the propellant surface and form agglomerates often orders of magnitude larger than the original particles [23]. Condensed phase agglomerates introduced into the exhaust gas decrease rocket motor performance due to lower than predicted exhaust gas temperatures and velocities [5]. Thermal and velocity lags in the exhaust gas can decrease theoretical predicted performance (I_{sp}) by as much as 3-5% [24]. Oxide caps (Al_2O_3) formed on the burning aluminum droplets and agglomerates contribute to high coarse fraction of alumina slag in exhaust products, further decreasing rocket performance [4]. Additionally, agglomerates flowing through the nozzle can cause internal structural damage to the motor resulting in mechanical and/or thermal failure of the rocket motor [25]. Utilizing mechanical activation to engineer reactive composite particles with lower ignition temperatures that could ignite more quickly than conventional aluminum has been shown to reduce agglomerate formations and potentially decrease two-phase losses and improve overall rocket performance [18, 25].

2.2 Mechanical Activation

Mechanical activation is an alternative approach to decrease the diffusion distance in micron scale reactive mixtures that does not suffer the drawbacks of replacing micron scale powders with nanoscale materials. Coarse aluminum fuel particles and polymer starting materials together with stainless steel grinding media are milled in high density polyethylene containers until an exothermic reaction is mechanically initiated and self-sustained combustion occurs. Reactive composite particles can be produced when this process is stopped (arrested) just prior to the exothermic reaction [2]. During milling, aluminum fuel particles are repeatedly fractured, deformed and cold welded by the grinding media, while the softer polymer powder coats the freshly exposed pure aluminum surfaces. The result of MA are reactive composite fuel particles comprised of thin layers of fuel material completely immersed in an polymer matrix that have modified reaction and combustion properties [26]. The improved reaction and ignition characteristics are achieved through increased interfacial contact of the reactants and decreases in diffusion distances exceeding those of nanoscale physical mixtures [2-4]. Both high and low energy milling techniques are utilized to produce reactive mixtures with altered ignition and combustion behavior for example the SPEX Mill 8000 vibratory shaker pictured in Figure 2.1 can be used when high intensity milling is desired resulting in shorter MA milling time. However inherent dangers with milling at high energy, particularly for large batches of materials (>1 gram), low energy milling techniques, such as roller milling may be preferred. Increased safety resulting from reductions in energy intensities of the grinding media on low intensity roller mills is ideal when milling very sensitive reactive mixtures or large scale batches because of energetics (Fig. 2.2). In addition to yielding composite particles with higher reactivity compared to physical mixtures of nanoscale materials the process is relatively simple, cost effective and easily scalable [27].



Figure 2.1. Spex Mill 8000 vibratory shaker mill.

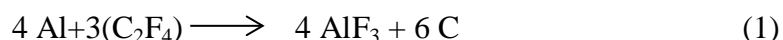


Figure 2.2. U.S. Stoneware roller mill.

2.3 Materials Selection

2.3.1 Polytetrafluorethylene Inclusion Material

Fluorocarbons such as polytetrafluoroethylene (C_2F_4) have been shown to have high specific heat associated with the fluorination of aluminum [16]. As such they may be utilized to replace traditional oxider materials in composite fuel particles. The fluorination of aluminum given by Equation (1) is accompanied by a gravimetric heat release of $2070 \text{ kcal}\cdot\text{kg}^{-1}$ [26].



The main product species from fluorination is aluminum fluoride (AlF_3) that sublimates at $1280 \text{ }^\circ\text{C}$ at 1 atm, instead of Al_2O_3 from oxidation ($T_{\text{Boil}} \approx 3000 \text{ }^\circ\text{C}$). This could result in less condensed phase products and potentially reduce two-phase losses in rocket motors. In addition to high heat release and potentially less condensed phase products, the sublimation of AlF_3 gas formed in the reactions could result in microexplosion of the particle due to increased internal pressurization [16]. Sippel et al. showed that agglomerate sizes could be reduced by adding 10-30 wt% PTFE inclusion material in composite fuel particles [16, 18]. They hypothesized two possible mechanisms for agglomerate size reductions: (1) Exothermic reactions of aluminum with PTFE reduces the particle residence time at the surface which decreases the possibility for the particle to coalesce and agglomerate, and (2) Gas production from PTFE decomposition and AlF_3 sublimation induce particle dispersion [4]. Al/PTFE reactions are highly exothermic and produce gas from AlF_3 sublimation and it may be difficult to determine if one mechanism is dominant. One way to assess this hypothesis is to investigate inclusion materials that will promote substantial gas generation with low heat release.

2.3.2 Low Density Polyethylene Inclusion Material

Low exothermicity and high gas production of Al/LDPE reactions indicate that LDPE inclusion material is a strong candidate to investigate gas induced microexplosions in mechanically activated fuel particles. Some reasons for low exothermicity and high gas production of Al/LDPE reactions with 10 wt% inclusion material have been discussed by Sippel et al. [19]. In summary, LDPE has a lower decomposition temperature (217 °C) compared to PTFE (473 °C) and yields fuel products of methane (CH₄) and carbon as opposed to strong oxidizing species of carbon tetrafluoride (CF₄), as with PTFE. Decomposition species have a strong effect on the exothermicity of Al/inclusion reactions and are tied to the adiabatic flame temperature. Despite the relatively low adiabatic flame temperatures of Al/LDPE reactions (305 °C), LDPE decomposition can still occur and results in significant gas production (6.99 g/mol). Although the adiabatic flame temperature of 90/10 wt.% Al/PTFE reactions is higher (1150 °C) it is not sufficiently high for AlF₃ sublimation (1280 °C) resulting in very little gas production for Al/PTFE reactions. Gas generation with very little heat release (-51.2 KJ/mol) compared to PTFE (-809 KJ/mol) make LDPE an ideal inclusion material to investigate the effectiveness of gas generation driven microexplosions.

3. MATERIALS PREPARATION AND EXPERIMENTAL APPARATUS

3.1 Materials Preparation and Milling

Batches of aluminum (Valimet H-30, 58 μm) / PTFE (Sigma Aldrich, 468096, 35 μm) particles were produced on a SPEX 8000M high energy mill. Batches of Al/LDPE (IASCO, LDP5, 500 μm) were produced on a US Stoneware CV-90116 low energy roller mill. Both materials were milled in argon-filled (99.997 vol.%) containers. Specifically, for production of Al/PTFE particles, manufacture was done using high energy milling of one gram batches and HDPE plastic milling containers (Cole Parmer EW-62201-01) were used for safety. A crash ratio of 24:1 was used with 440C steel media (McMaster Carr (5) 3/8" dia. and (15) 3/16" dia.) and batches were milled with a duty cycle of 1 minute ON and 4 minute OFF while being cooled continuously by a fan for milling durations of either 20 min or 60 min. As Al/LDPE particle manufacture is potentially less hazardous than Al/PTFE manufacture, a scaled manufacturing technique was used to produce Al/LDPE particles. Aluminum/LDPE particles were produced via low energy roller milling in 200 g batches in a one-gallon argon-filled HDPE container (6 inch Diam.) at a crash ratio of 70:1 and a rotational speed of 90 RPM for 52 hours. All materials were handled in an argon filled glove box after milling and covered with hexane. The hexane was allowed to slowly evaporate and the passivated material was sieved to $> 75 \mu\text{m}$. The appropriate milling duration of the scaled low energy manufacturing technique used to produce Al/LDPE particles was selected by matching DSC heat release characteristics from low energy milled particles to those of similar Al/LDPE particles milled for 60 min using the high energy manufacturing technique described previously.

Prior to ignition experiments, a Hirox KH-8700 digital optical microscope was used to image the particles and determine the top surface area of each particle used in experiments. Particles used in experiments were thin and flat in morphology. As only the top surface area of a particle is exposed to laser radiation, the equivalent cross-sectional diameter of single particles was used in measurements and was calculated as

$$D_{Eq,CSA} = \left(\frac{4}{\pi} SA_{Top}\right)^{\frac{1}{2}} \quad (2)$$

where SA_{Top} is the microscope measured top surface area of the particle.

3.2 Morphology and Microstructural Characterization of Al/PTFE and Al/LDPE

Chemical mapping (EFTEM) was performed to confirm that Al and polymer inclusions co-exist in a single composite particle. Although EFTEM can be useful in elemental mapping at the nanoscale, SSI analysis was used to generate mass-thickness contrast images to characterize the three-dimensional structure and morphologies of the composite particles (Fig. 2). In these images, layered structures formed by the stacking of Al flakes are shown. The Al flakes are transparent to the TEM having a thickness on the order of 50-100 nm. Based on the observations from EFTEM mapping and SSI imaging, it can be concluded that the polymer is well penetrated into the layered structure of the Al, filling gaps between Al layers. Mechanical activation of Al/polymer mixtures results in the formation of a hybrid flake Al particle with plate-like morphology held together and protected from oxidation by the inclusion materials, which is consistent with morphological properties of MA Al/polymer particles described in previous work by Sippel *et al.* [27]. The images also show that the composite particles processed with PTFE or LDPE have similar microstructures and the mechanism of microexplosions in reactive (PTFE) or non-reactive (LDPE) composite polymer particles can be explored.

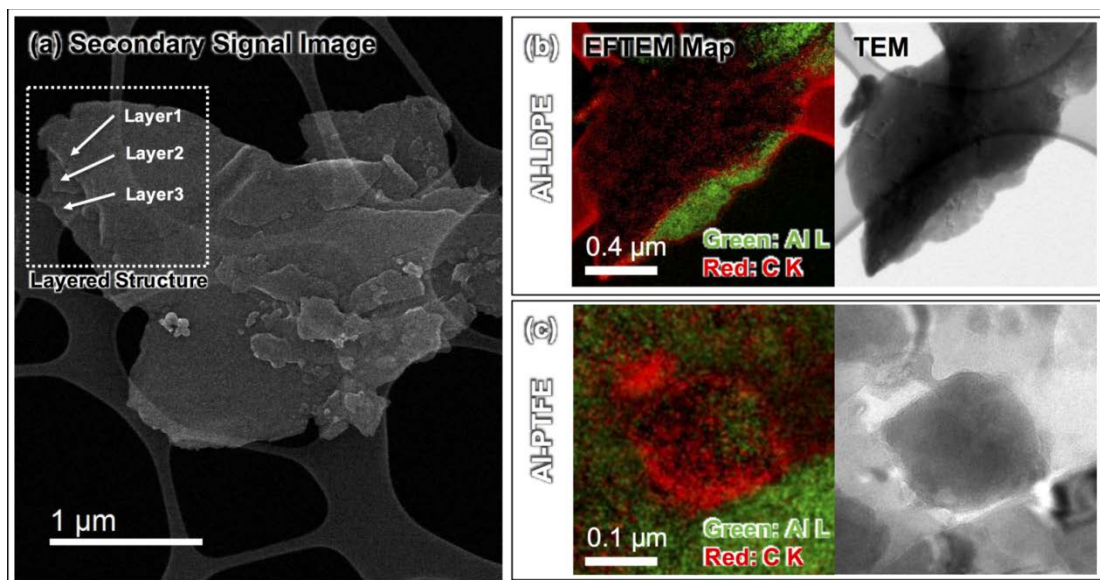


Figure 3.1. Representative secondary signal image of an Al-LDPE particle (a) EFTEM composite maps and TEM images of (b) Al/LDPE (90/10 wt.% 52 hr MA) and (c) Al/PTFE (70/30 wt.%, 60 min MA).

3.3 Single Particle Ignition Experiments

Contrary to previous studies in which bulk ignition characteristics are identified for aerosolized powder flows [5,18-21], loose powders [22] and densified compositions [23], in this work we study single particle ignition in order to observe intraparticle dynamics. Further, to mimic the combined conductive-radiative thermal environment at a solid-gas reaction interface, single particles are irradiated on a ceramic substrate (OZM Research, FSK 50-20K).

A Coherent GEM 100A, 10.6 μm wavelength, 100 W CO₂ laser was used to heat single particles of composite materials with equivalent cross-sectional diameters ($D_{Eq,CSA}$) ranging from 100-1200 μm. The laser energy profile has a Gaussian distribution across the beam with the peak irradiance at the center of the beam. A ThorLabs ZnSe plano convex lens (500 mm focal length) was used to focus the laser beam to a $1/e^2$ diameter of 2.6 mm for experiments for laser flux between 78-600 W/cm² and 0.6 mm for experiments between 2400-7700 W/cm². LabVIEW was used to control the laser power output and pulse time. The power output of the laser was measured with a Coherent

LabMax TOP, laser power and energy meter and a high laser flux ($> 9000 \text{ W/cm}^2$) was used to mark the incident beam location on the ceramic tile prior to experiments. The composite fuel particles were placed in the center of the incident beam location.

A high-speed Vision Research Phantom v7.3 video camera equipped with a long distance microscopic optic (Infinity Photo-Optical K2 lens) was used to observe the reaction of the laser heated particles (Fig. 3.2.). The camera was triggered at the beginning of the laser pulse time and the recorded videos were used to determine “first light” ignition delay, defined as the time lapse from the start of sample irradiation to the first presence of reaction emission as has been done previously by others [26]. A $335 \pm 55 \mu\text{s}$ time delay between the LabVIEW control panel and laser onset as well as the laser manufacturer specified laser rise time ($95 \pm 5 \mu\text{s}$) were subtracted from measured ignition delay times. The composite particles, laser flux and camera settings used for experiments are summarized in Table 3.1.

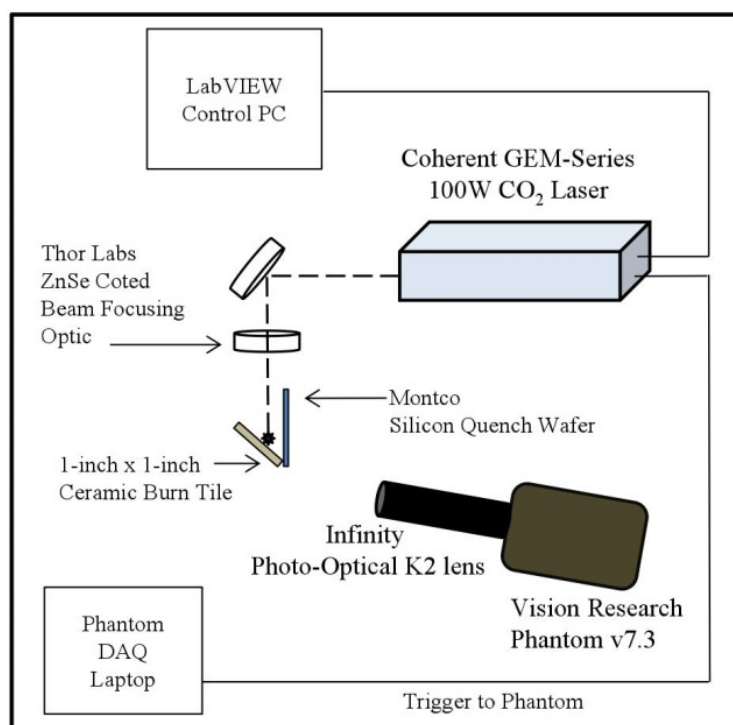


Figure 3.2. Schematic of the experimental apparatus for ignition experiments and product collection.

Table 3.1. Heating flux and camera settings for ignition experiments.

Material	Laser Flux (W/cm ²)	Camera Frame Rate (fps)	Exposure (μs)
70/30 Al/PTFE	78	1200	830
20 minute MA	150-600	11,000	10
70/30 Al/PTFE	78	1200	830
60 minute MA	150-600	11,000	10
90/10 Al/PTFE	600	11,000	89
60 minute MA	2400-7700	30,000	15
90/10 Al/LDPE	2400-7700	30,000	20
52 hr MA			

3.4 Product Size Distributions

Reaction products were collected for post-combustion analysis on one-inch square silicon (Si) wafers, prepared by cutting Montco Silicon, P/Boron orientation type, 500 mm thick, 100 mm diameter wafers (Fig. 3.2). Size distributions of the reaction products were determined for 70/30 wt.% Al/PTFE (20 and 60 min MA) for laser fluxes of 200 and 500 W/cm², 90/10 wt.% Al/PTFE (60 min MA) and 90/10 wt.% Al/LDPE (52 hr MA) at a laser flux of 5800 W/cm². Remaining products on both the ceramic tile where particle heating occurred and the Si quench surface were imaged via a Hirox KH-8700 digital microscope equipped with a OL-700 II Objective lens and NR-450-OL ring light. ImageJ (NIH) software was used to post-process the images and determine the product particle size distributions.

4. RESULTS AND DISCUSSION

4.1 Al/PTFE 70/30 wt.% (20, 60 min MA)

Typical results of combustion experiments are presented as image sequences in Fig. 4.1 and show microexplosion events at laser fluxes in excess of 150 W/cm^2 . The minimum ignition threshold for 20 min. milled 70/30 wt.% Al/PTFE was between 60-78 W/cm^2 and a similar threshold was observed for 60 min. milled particles. At 78 W/cm^2 laser flux, some particles did not ignite and simply expanded without significant light emission as a result of PTFE degradation (Fig. 4.1(a)). Observed particle expansion in experiments with low laser fluxes are consistent with the microstructure of the plate-like particles consisting of layered Al flakes bound together with polymer inclusion material.

At higher heating fluxes ($>150 \text{ W/cm}^2$), the ignition delays are much shorter due to more rapid gas production leading to higher internal pressurization. This causes the particles to microexplode and shatter into smaller fragments (Fig. 4.1(b) and (c)). For high flux (600 W/cm^2) experiments, intraparticle reaction is sufficiently prompt that particle ejection is observed after first light is observed. Initially, it was expected that 60 min. milled particles would be more reactive and would exhibit more microexplosions due to greater microstructural refinement and more intimate mixing of constituent materials at longer milling durations [16]. However, contrary to expectations, very little difference is observed in the combustion dynamics or ignition behavior with increasing milling time and there does not appear to be a significant ignition benefit in particle modification with longer milling duration. Although some 60 min. MA microexplosion products (21 vol.%) were between 45-50 μm , 80 vol.% of ejecta particles are smaller than 30 μm (Fig. 4.2). Size distribution of products from 20 min. milled Al/PTFE show that all ejecta particle sizes are smaller than 30 μm indicating that short milling durations are

sufficient to effectively alter the microstructure of composite fuel particles. Though as-milled particles are more flake-like in morphology and contain polymer contributions, the equivalent diameter of these particles (250-500 μm) are quite large in comparison to the actual diameter of combustion products. These results are in agreement with qualitative results of previous studies using similar composite particles in composite solid propellants [15] and indicate microexplosion of composite particles with large equivalent diameters can result in combustion products of small diameter.

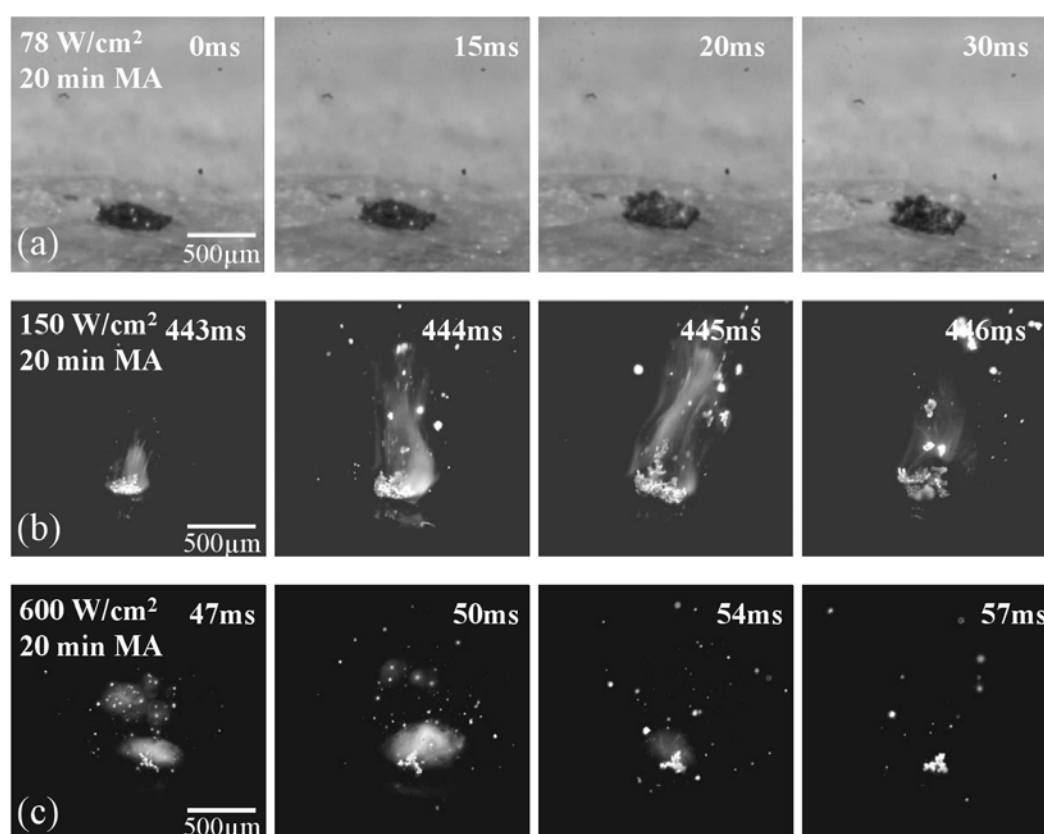


Figure 4.1. Image sequences captured from laser ignition of a single 70/30 wt.% Al/PTFE 20 min. MA particle, indicating the effect of laser flux: (a) 78 W/cm^2 , no-ignition (b) 150 W/cm^2 , microexplosion, and (c) 600 W/cm^2 , microexplosion.

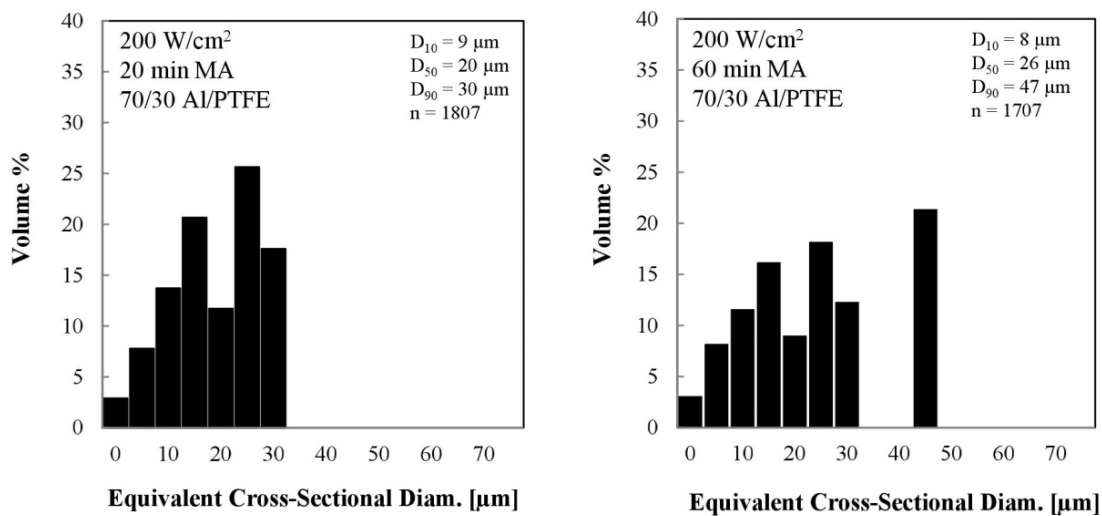


Figure 4.2. Product particle size distributions for 70/30 wt.% Al/PTFE as a function of laser flux and mechanical activation duration.

Initial particle size influences the intensity of microexplosions (Fig. 4.3). Particles with larger equivalent diameter exhibit more vigorous reactions, resulting in greater fragmentation and large jetting flames. This is expected as larger particles promote higher internal pressure rise as gases need to diffuse out longer distances. On average, smaller initial particle size results in smaller fragment sizes, lower number of fragments and smaller jets suggesting lower pressurization.

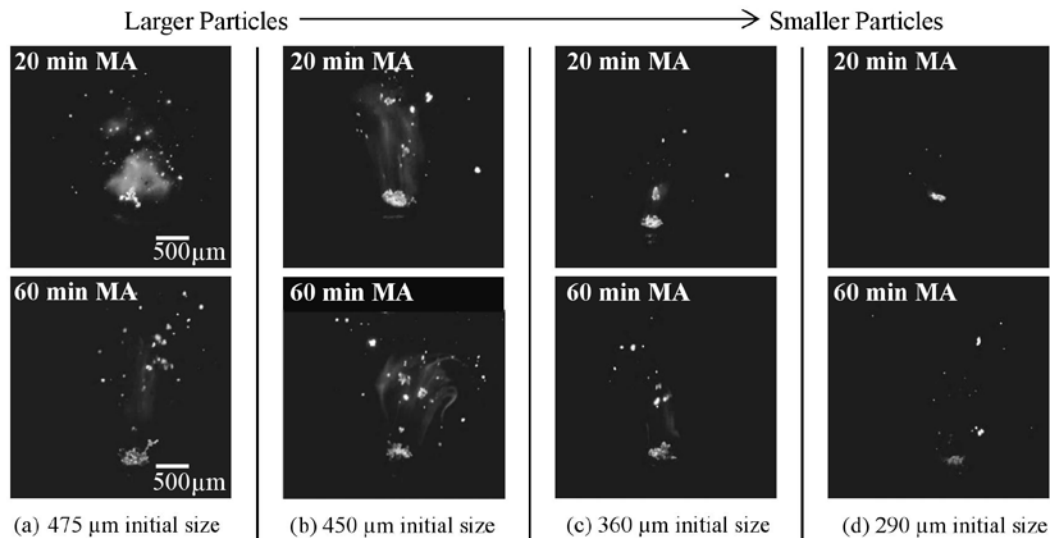


Figure 4.3. Initial particle size effect on microexplosion of composite fuel particles for 70/30 wt.% Al/PTFE 20 and 60 min MA at 600 W/cm^2 for approximate . equivalent cross-sectional diameters of (a) $475 \mu\text{m}$ (b) $450 \mu\text{m}$ (c) $360 \mu\text{m}$ (d) $290 \mu\text{m}$.

Quantifying the ignition delay for reactive particles is important as it defines a particle's transition from being a heat sink to a heat source [28]. Ignition delays are determined for each experiment (ten experiments at each laser flux) and are reported as a function of particle size for both 20 and 60 min. MA particles (Fig. 4.4(a)). The ignition delay and standard deviation are presented in Fig. 4.4(b). The ignition delays decrease with higher laser flux for both 20 min MA and 60 min MA particles. The milling duration (either 20 or 60 min MA) has little effect on ignition delay time for all laser fluxes (Fig. 4.4(b)) suggesting that 20 min MA is sufficient to alter particle ignition. Particles heated with the highest laser flux (600 W/cm^2) considered have the shortest ignition delay times of 40 ms and 34 ms for 20 min MA and 60 min MA respectively. No clear particle size dependence is observed for the ignition delay for either 20 min MA or 60 min MA particles at the size range used in experiments. This is not surprising because for plate-like morphology particles, the incident heat flux and particle volume vary at the same rate, and volumetric heating rates would be nearly identical for different sized particles. Ignition delays are slightly longer only at low flux (150 W/cm^2) for 60 min. milled Al/PTFE compared to 20 min. milled particles. At this low laser flux the variation in ignition delay does appear to be flux dependent for 60 min. milled Al/PTFE.

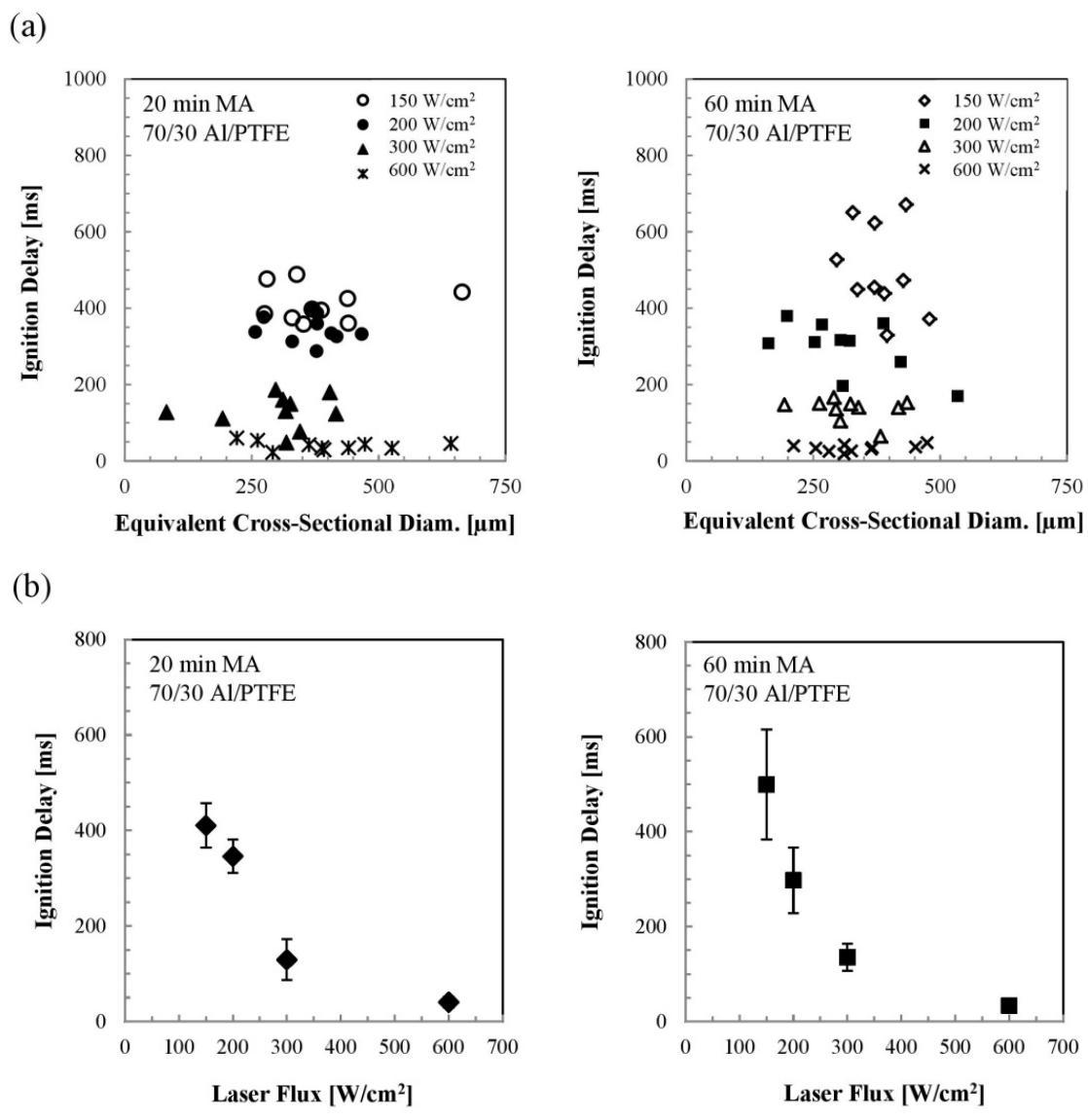


Figure 4.4. Ignition delays of 70/30 wt.% Al/PTFE milled for 20 and 60 min MA as a function of (a) equivalent and (b) laser flux.

4.2 Al/PTFE 90/10 wt.% (60 min MA)

Decreasing inclusion content to 10 wt.% significantly alters the ignition and reaction dynamics of the composite particles. The ignition threshold is much higher compared to 70/30 wt.% Al/PTFE. For example, with a laser flux of 600 W/cm^2 , 90/10 wt.% particles produce no ejecta (Fig. 4.5(a)). The gas production is too slow to result in pressure build up and outgassing occurs. In contrast, high gas production and microexplosions were observed from ignition of 70/30 wt.% particles at this flux. Microexplosions from 90/10 wt.% Al/PTFE particles are only observed at and above 2.4 kW/cm^2 laser flux (Fig. 4.5(b)), which is much higher than the microexplosion threshold for particles with 30 wt.% PTFE (150 W/cm^2), indicating that rapid self-heating due to Al/PTFE reaction is the primary cause of microexplosions. Few ejecta are observed at this threshold level, but at a higher laser flux (7.7 kW/cm^2), more microexplosions accompanied by jetting flames are observed due to faster heating (Fig. 4.5(c)). In experiments with laser flux at and above 2.4 kW/cm^2 , aluminum droplets burning with a characteristic oxide cap are observed after the occurrence of microexplosions (Fig. 4.5(b)(c)). From the observation of aluminum and substrate melting, bulk particle heating rates of experiments conducted at 7.7 kW/cm^2 can be estimated to be $\sim 10^5 \text{ K/s}$, which is similar to estimated aluminum particle heating rates within solid rocket motors [5].

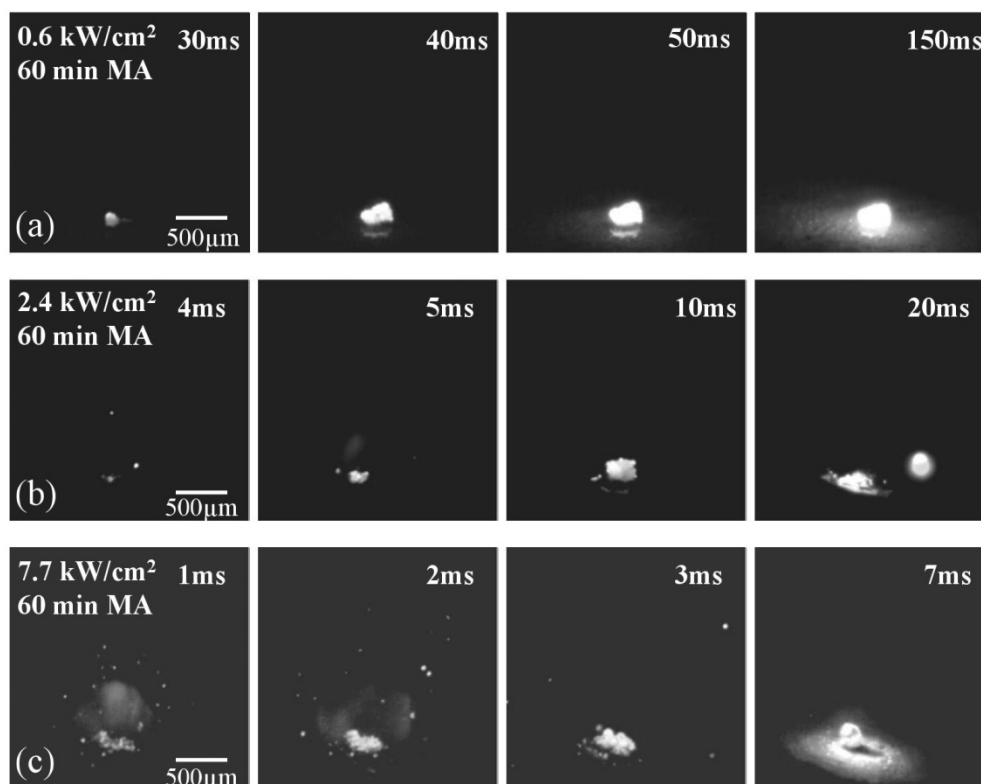


Figure 4.5. Image sequences of the reaction dynamics of 90/10 wt.% Al/PTFE 60 min MA for laser fluxes of (a) 0.6 kW/cm² (b) 2.4 kW/cm² and (c) 7.7 kW/cm².

The results from ten experiments at each laser flux are reported as a function of particle size (Fig. 4.6(a)) and the ignition delay and standard deviation are reported as a function of laser flux (Fig. 4.6(b)). Results suggest the presence of two distinct ignition mechanisms for composite particles: (1) size-independent prompt ignition due to intra-particle reactions at high laser flux and (2) weakly size-dependent reaction at lower flux. Similar to 70/30 wt.% Al/PTFE, at high laser flux (7.7 kW/cm²), ignition delay of 90/10 wt.% Al/PTFE is not dependent upon particle size. However, at lower laser fluxes, ignition delay is weakly dependent upon particle size and appears to be bimodal. The weak size dependence of the ignition delay for 90/10 wt.% Al/PTFE particles is expected to be an effect of the overall lower PTFE content resulting in lower Al/PTFE reaction heat release. Ignition can rapidly occur within a particle due to the nanostructure for both higher PTFE content particles (70/30 wt.% Al/PTFE) and at higher heating fluxes.

However, at low flux and with lower PTFE content, intraparticle heating is not sufficient to produce prompt ignition required for internal pressurization. Instead, particles heat in bulk with slower polymer decomposition until they eventually reach the bulk aluminum ignition temperature.

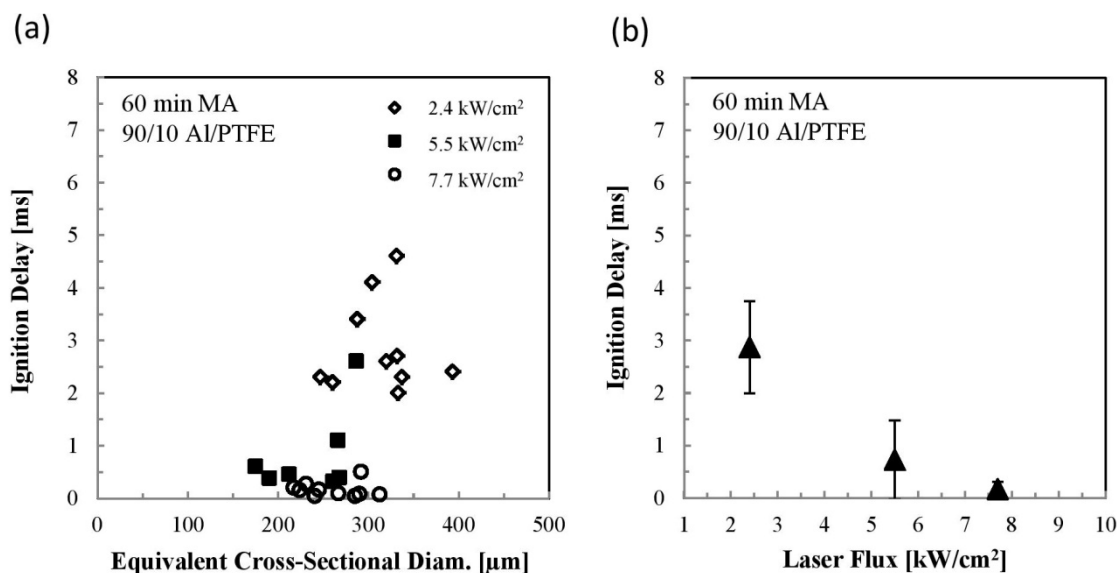


Figure 4.6. (a) Ignition delay of 90/10 wt.% Al/PTFE (60 min MA) for laser fluxes of 2.4, 5.5 and 7.7 kW/cm², (b) average ignition delay as a function of laser flux (Al/PTFE 90/10 wt.%).

Combustion products for 90/10 Al/PTFE at 5.8 kW/cm² are predominantly comprised of products within the size range of 30-40 μm (Fig. 4.7(a)). The resulting particle size distribution is similar to that for 70/30 Al/PTFE at a lower flux (Fig. 4.7(b)) with additional contributions present from particles between 30-40 μm . Despite contributions from a few larger particles resulting from quenched Al droplets (30-40 μm , images not shown), the overall reduction in product sizes from 150-400 μm (pre-ignition) to less than 40 μm (post-ignition) is significant. Results show that the addition of just 10 wt.% PTFE can still result in fuel particles that disperse at high heating rates typically encountered in propellants ($\sim 10^5$ K/s).

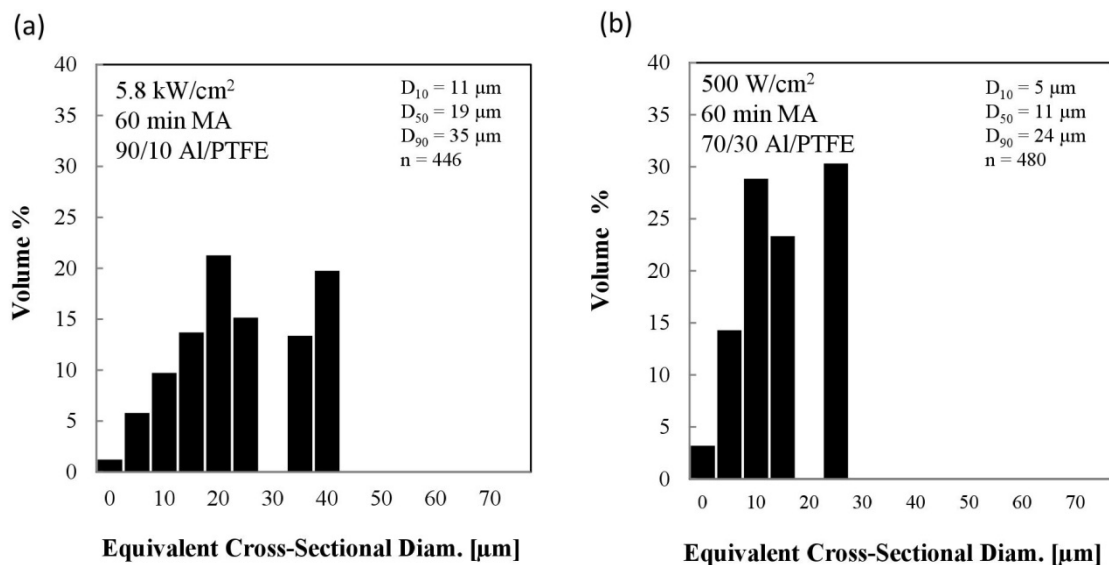


Figure 4.7. Product particle size distribution for (a) 90/10 wt.% Al/PTFE (60 min MA) at 5.8 kW/cm² laser flux and (b) 70/30 wt.% Al/PTFE (60 min MA) at 500 W/cm² laser flux

4.3 Al/LDPE 90/10 wt.% (52 hr MA)

It is expected that critical heating thresholds required for microexplosion would be higher for Al/LDPE particles than Al/PTFE particles due to the low exothermicity of Al and LDPE reactions. The LDPE decomposition species (mainly CH₂ and C) are not expected to react strongly with Al, but the higher gas production of LDPE as compared to PTFE inclusion material may be sufficient to break apart the particle, exposing more Al surfaces. In experiments at or below a laser flux of 2.4 kW/cm², the particles are observed to glow and slowly release gas as they thermally expand due to LDPE decomposition (Fig. 4.8(a)). However, at higher laser heating flux experiments (5.5 kW/cm²), a critical microexplosion threshold is observed. At this flux only, minimal particle dispersion is observed and a hydrocarbon flame followed by significant particle expansion results ending with Al droplets burning (Fig. 4.8(b)). Analysis of videos at this flux shows that in some cases, LDPE may not completely vaporize and large particles of combustion products (~100-200 μm) remain after weak microexplosions have occurred. At higher laser flux (7.7 kW/cm²), microexplosions are much more vigorous and clouds of small ejecta can be seen igniting in air above the particle (Fig. 4.8(c)).

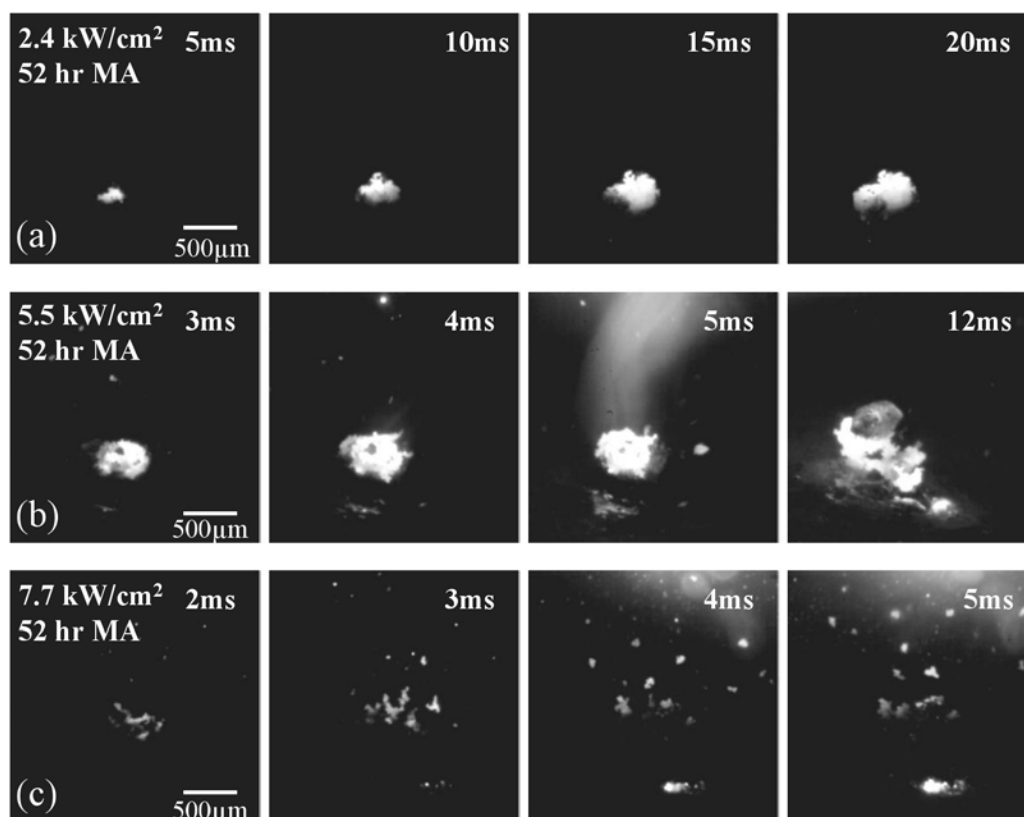


Figure 4.8. Image sequences capturing reaction dynamics of laser heated 90/10 wt.% Al/LDPE (52 hr MA): (a) 2.4 kW/cm², (b) 5.5 kW/cm², and (c) 7.7 kW/cm² laser fluxes.

The ignition delays from ten experiments at each heating flux are reported as a function of particle size (Fig. 4.9(a)) as well as the ignition delay and standard deviations at each laser flux level (Fig. 4.9(b)). Similar to 90/10 wt.% Al/PTFE particles, ignition delay for Al/LDPE (90/10 wt.%) particles does appear to depend on particle size at lower laser fluxes (2.4 kW/cm²). Due to low Al/LDPE reaction exothermicity, Al/LDPE particles behave similarly to 90/10 wt.% Al/PTFE particles ignited at low laser fluxes. Much larger contributions from coarse products were seen with 90/10 wt.% Al/LDPE (Fig. 4.10) as compared to 90/10 wt.% Al/PTFE (60 min MA) product distributions at the same heating flux (Fig. 4.7(a)) as expected from analysis of the ignition videos. Results from product collection of Al/LDPE fragments near the microexplosion threshold (5.8 kW/cm²) show 95 vol.% contribution from coarse particles, ranging from 40-170 μm (Fig. 4.10), with the majority of particle fragments being larger than ~160 μm. Additionally,

there is a more pronounced difference in fine to coarse product particle size with 90/10 wt.% Al/LDPE as compared to Al/PTFE product particle sizes. Overall, the product particle sizes were much smaller than the equivalent diameters of neat Al/LDPE particles, showing that gas production alone, without the presence of strong intraparticle reactions, is enough to induce microexplosion at high heating rates. This is consistent with previous agglomeration studies in which microexplosions were observed in both Al/PTFE and Al/LDPE particle heating within burning composite solid propellants and shows that either type of inclusion modified particle can be effective [16,17]

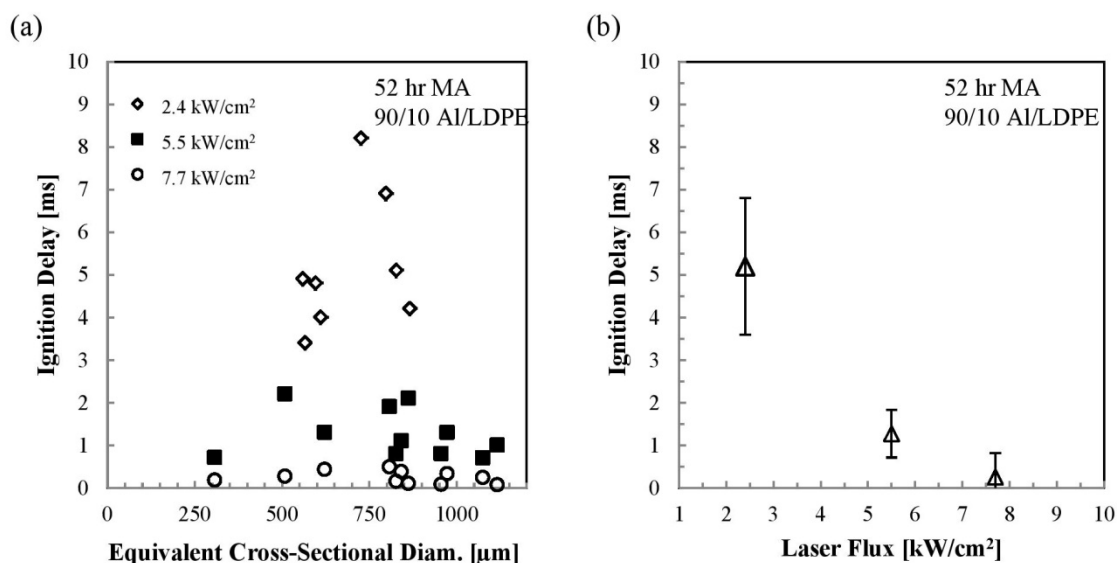


Figure 4.9. Ignition delay of 90/10 wt.% Al/LDPE (52 hr MA) at 2.4, 5.5 and 7.7 kW/cm² laser flux as a function of (a) equivalent diameter and (b) laser flux.

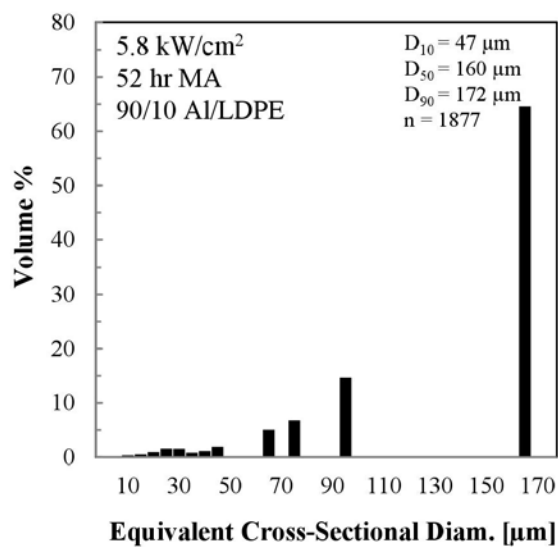


Figure 4.10. Product particle size distribution of 90/10 wt.% Al/LDPE 52hr MA at 5.8 kW/cm² laser flux.

5. CONCLUSIONS

Overall this work provides an initial understanding of how particle composition/structure, particle size, and laser flux affect the ignition time and reaction dynamics of engineered composite particles. Microexplosions were observed for both Al/PTFE and Al/LDPE composite particles and the resulting product particle sizes were much smaller than neat particle sizes. Microexplosion tendency was found to be dependent upon laser flux and indicates that the presence of PTFE inclusions reduces this threshold due to self-heating from Al/PTFE reaction.

Although all 70/30 wt.% Al/PTFE particles above the critical ignition energy threshold (78 W/cm^2) microexploded, it appeared that larger particles ($>360 \mu\text{m}$) reacted more vigorously, breaking into more pieces than smaller particles and had ejecta with flake-like morphology. This suggests that for engineered Al/polymer composite particles, larger particles may be as effective or more effective than smaller particles at reducing agglomerate size. For particles with 30 wt.% PTFE, Microexplosions occurred at lower laser fluxes and particles exhibited high gas production and violent particle dispersion. In contrast, composite particles having only 10 wt.% PTFE were only observed to microexplode at very high heating fluxes ($>2.4 \text{ kW/cm}^2$). Although microexplosions were more prominent at higher heating flux for this material, spherical aluminum droplet combustion was also observed for some conditions. The polymer inclusion content is critical to producing microexplosions, as exothermic reactions between aluminum and PTFE act to facilitate rapid, localized heating.

Aluminum/inclusion heat release and laser flux are critically important to ignition delay. For particles with 30 wt.% PTFE, ignition delay is found to be nearly independent of particle size for all laser fluxes explored, suggesting that particle ignition for laser fluxes investigated is controlled by intra-particle reaction of nanoscale inclusions with aluminum. For engineered particles containing only 10 wt.% PTFE or LDPE, two ignition mechanisms were observed. Both size-independent, inclusion-controlled ignition and size-dependent ignition delay scaling were observed. Such dependence upon diameter is akin to bulk aluminum particle ignition and is attributed to the absence of strong, intra-particle reactions and absence of strong intraparticle pressurization.

Al/PTFE (90/10 wt.%) particles were found to produce much smaller combustion product fragments (~1-40 μm) than Al/LDPE (90/10 wt.%) particles (~10-160 μm) at similar heating flux. However, considering the very large starting size range of Al/LDPE particles (~250-1200 μm), microexplosion of Al/LDPE composite fuel particles could significantly reduce agglomerate sizes in energetic material applications, as was observed in solid propellants elsewhere [17].

Contrary to expectations, milling duration does not appear to have a significant effect on ignition delay for the conditions considered here, as it is expected that particle nanostructure developed from short duration milling (i.e. 20 min MA) is sufficient to alter particle ignition significantly. This work shows milling durations well below the critical ignition time are sufficient to produce microexplosions, which could improve the safety of scaled up particle manufacture. This effort indicates that in high heating rate environments, either oxidizer or fuel polymer inclusions may lead to good particle dispersion and shorter ignition delay, but in lower heating rate environments, Al/PTFE exhibits better dispersion and shorter ignition delay due to intra-particle reactivity. These results provide guidelines for design of nanostructured Al/polymer fuel particles for energetic materials applications.

LIST OF REFERENCES

1. L. Meda, G. Marra, L. Galfetti, F. Severini & L. De Luca. Nano-Aluminum as Energetic Material for Rocket Propellants. *Materials Science and Engineering*, 27, 1393-1396 (2007).
2. E.L. Dreizin (2009). Metal-Based Reactive Nanomaterials. *Progress in Energy and Combustion Science*, 35(2), 141-167 (2009). Doi:10.1016/j.pec.2008.09.001.
3. M.W. Beckstead, Correlating aluminum burning times, *Combustion Explosion and Shock Waves* 41 (2005) 533-546.
4. K.V. Anand, A. Roy, I. Mulla, K. Balhudhe, K. Jayaraman & S.R. Chakravarthy. Experimental Data and Model Predictions of Aluminum Agglomeration in Ammonium Perchlorate-Based Composite Propellants Including Plateau-Burning Formulations. *Proceedings of the Combustion Institute*, 34, 2139-2146 (2013).
5. R.L. Geisler. A Global View of the Use of Aluminum Fuel in Solid Rocket Motors. *AIAA/ASME/SAE/ASEE Joint Propulsion Conference*, (2002).
6. M.A. Trunov, M. Shoenitz & E.L. Dreizin. Ignition of Aluminum Powders Under Different Experimental Conditions. *Propellants, Explosives and Pyrotechnics*, 30, (2005).
7. K. Jayaraman, S.R. Chakravarthy & R. Sarathi. Accumulation of Nanoaluminum During Combustion of Composite Solid Propellant Mixtures. *Combustion, Explosion and Shock Wave*, 46, 21-29 (2010).
8. R.A. Yetter, G.A. Risha & S.F. Son. Metal Particle Combustion and Nanotechnology. *Proceedings of the Combustion Institute*, 32, 1819-1838 (2009).
9. L.T. De Luca, L.G. Galfetti, G.O. Colombo, F. Maggi & A. Bandera. Microstructure Effects in Aluminized Solid Rocket Propellants. *Journal of Propulsion and Power*, 26 (2010).
10. D.T. Bui, A.I. Atwood, T.M. Antienza-More, Effect of aluminum particle size on combustion behavior of aluminized propellants in PCP binder, in: 35th International Annual Conference of ICT, Karlsruhe, (2004).
11. O. Orlandi, J.F. Guery, G. Lacroix, S. Chevalier, N. Desgardin, HTPB/AP/Al Solid propellants with nanometric aluminum, in: European Conference for Aerospace Sciences (EUCASS), Moscow, (2005).

12. V.N. Simonenko, V.E. Zarko, Comparative study of the combustion behavior of composite 0.propellants containing ultrafine aluminum, Proc. 30th Annual Conference of ICT (1999).
13. D.A. Yagodnikov, E.A. Andreev, V.S. Vorob'ev, E.A. Andreev and O.G. Glotov. Ignition, Combustion and Agglomeration of Encapsulated Aluminum Particles in a Composite Solid Propellant I: Experimental Studies of Agglomeration. *Combustion, Explosion and Shockwave*, 42(5), 534-542 (2006).
14. O.G. Glotv, D.A. Yagodnikov, V.S. Vorob'ev, V.E. Zarko & V.N. Simonenko. Ignition, Combustion and Agglomeration of Encapsulated Aluminum Particles in a Composite Solid Propellant II: Experimental Studies of Agglomeration. *Combustion, Explosion and Shockwaves*, 43(3), 320-333 (2007).
15. T.R. Sippel, S.F. Son & L.J. Groven (2014). Aluminum Agglomeration Reduction in a Composite Propellant Using Tailored Al/PTFE Particles. *Combustion and Flame*, 161, 311-321 (2014).
16. T.R. Sippel, S.F. Son, & L.J. Groven. Altering Reactivity of Aluminum with Selective Inclusion of Polytetrafluoroethylene through Mechanical Activation. *Propellants, Explosives and Pyrotechnics*, 35, 1-10 (2012).
17. S. Zhang, M. Shoentiz, E.L. Dreizin, Metastable aluminum based reactive composite materials prepared by cryomilling, 50th AIAA Aerospace Sciences Meeting (2012).
18. Y. Shoshin, E.L. Dreizin, Laminar lifted flame speed measurements for aerosols of metals and mechanical alloys, *AIAA Journal* 42 (2004) 1416-1426.
19. Y. Huang, G.A. Risha, V. Yang, R.A. Yetter, Effect of particle size on combustion of aluminum particle dust in air, *Combust. Flame* 156 (2009) 5-13.
20. G.A. Risha, R.A. Yetter, V. Yang, Experimental investigation of aluminum particle dust cloud combustion, 43rd AIAA Aerospace Sciences Meeting and Exhibit (2005).
21. S. Mohan, M.A. Trunov, E.L. Dreizin, Heating and ignition of particles by a CO₂ laser, *J. Propul. Power* 24(2) (2008) 199-205.
22. J.J. Granier, M.L. Pantoya, laser ignition of nanocomposite thermites, *Combust. Flame* 138 (2004) 373-383.

23. J.J. Granier, T. M. Mullen, M.L. Pantoya, Nonuniform laser ignition in energetic materials, *Combust. Sci. Technol.* 175 (2003) 1929-1951.
24. L.T. DeLuca, C. Paravan, A. Reina, E. Marchesi, Aggregation and incipient agglomeration in metallized solid propellants and solid fuels for rocket propulsion, *AIAA/ASME/SAE/ASEE Joint Propulsion Conference* (2010).
25. E.W. Price, J.E. Crump, H.C. Cristensen, R. Sehgal, Comments on alumina size distributions from high-pressure composite solid-propellant combustion, *AIAA Journal* 3 (1965).
26. K. Moore, M.L. Pantoya, S.F. Son, Combustion behaviors resulting from bimodal aluminum size distributions in thermites, *J. Propul. Power* 23(1) (2007) 181-185.
27. T.R. Sippel, S.F. Son, L.J. Groven, Altering reactivity of aluminum with selective inclusion of polytetrafluoroethylene through mechanical activation, *Propellants Explosives and Pyrotechnics* 38 (2013) 286-295.
28. T.S. Ward, M.A. Trunov, M. Schoenitz, E.L. Dreizin, Experimental methodology and heat transfers model for identification of ignition kinetics of powdered fuels, *Int. J. Heat Mass Transfer* 49 (2006) 4943-4954S. Zhang, M. Shoentiz & E.L. Dreizin. Metastable Aluminum Based Reactive Composite Materials Prepared by Cryomilling. *50th AIAA Aerospace Sciences Meeting*, (2012).

APPENDIX A. DATA TABLES OF RESULTS FROM IGNITION EXPERIMENT

Table A.1. Results from laser ignition experiments for 70/30 Al/PTFE 20 min MA.

<i>Laser Flux (W/cm²)</i>	<i>Test #</i>	<i>Particle D_{eq,SA} (μm)</i>	<i>T_{ign delay} (ms)</i>
150	1	338.5	488.5
	2	275.1	385.6
	3	279.8	476.6
	4	368.8	397.6
	5	329.6	374.9
	6	438.7	425.5
	7	351.9	358.5
	8	664.4	442.3
	9	386.7	394.9
	10	440.2	360.9
200	1	378.7	359.7
	2	406.5	334.6
	3	466.5	332.5
	4	273.4	376.6
	5	256.7	337.9
	6	368.3	400.9
	7	377.5	287.7
	8	417.1	326.2
	9	329.6	313.1
	10	379.0	387.5
300	1	297.0	186.5
	2	316.8	130.6
	3	82.0	127.7
	4	318.2	48.0
	5	311.4	160.3
	6	415.9	123.9
	7	344.9	76.8
	8	326.0	149.7
	9	192.5	111.2
	10	403.8	179.8

Table A.1. Continued

600	1	440.6	34.6
	2	392.1	29.3
	3	472.8	43.6
	4	291.4	22.6
	5	261.4	54.1
	6	388.1	34.8
	7	642.3	45.8
	8	220.4	60.2
	9	526.1	33.8
	10	362.8	42.4

Table A.2. Results from laser ignition experiments for 70/30 Al/PTFE 60 min MA.

<i>Laser Flux (W/cm²)</i>	<i>Test #</i>	<i>Particle D_{eq,SA} (μm)</i>	<i>T_{ign delay} (ms)</i>
150	1	295.9	527.5
	2	370.8	623.7
	3	478.7	371.8
	4	432.3	671.5
	5	336.8	449.5
	6	327.6	650.9
	7	389.8	438.8
	8	370.3	455.3
	9	427.2	473.3
	10	395.0	329.5
200	1	388.1	360.6
	2	198.1	379.9
	3	266.9	357.3
	4	307.8	196.6
	5	422.2	259.7
	6	534.2	170.1
	7	321.4	314.9
	8	161.5	308.3
	9	252.7	311.4
	10	303.6	316.8
300	1	261.7	150.6
	2	323.2	149.4
	3	294.5	136.0
	4	338.9	140.6
	5	417.4	139.9
	6	382.3	64.9
	7	193.0	147.3
	8	434.7	152.9
	9	290.4	166.5
	10	302.9	104.6
600	1	325.2	26.3
	2	474.2	47.8
	3	254.9	33.6
	4	280.9	25.3
	5	364.3	31.2
	6	451.5	36.7
	7	310.5	18.5
	8	366.1	35.1
	9	211.4	39.6
	10	311.1	42.3

Table A.3. Results from laser ignition experiments for 90/10 Al/PTFE 60 min MA.

<i>Laser Flux (W/cm²)</i>	<i>Test #</i>	<i>Particle D_{eq,SA} (μm)</i>	<i>T_{ign delay} (ms)</i>
2400	1	393.0	2.41
	2	303.9	4.11
	3	336.9	2.31
	4	319.7	2.61
	5	260.2	2.21
	6	287.4	3.41
	7	246.6	2.31
	8	331.0	4.61
	9	331.6	2.71
	10	332.7	2.01
5500	1	382.0	2.61
	2	286.3	0.18
	3	-	-
	4	265.0	1.11
	5	266.0	0.33
	6	260.7	0.61
	7	174.8	0.39
	8	190.1	0.4
	9	267.5	0.46
	10	211.9	0.44
7700	1	0.54	0.05
	2	0.54	0.05
	3	0.57	0.08
	4	0.58	0.09
	5	0.59	0.1
	6	0.65	0.16
	7	0.77	0.28
	8	0.66	0.17
	9	0.7	0.21
	10	1	0.51

Table A.4. Results from laser ignition experiments for 90/10 Al/LDPE 52 hr MA.

<i>Laser Flux (W/cm²)</i>	<i>Test #</i>	<i>Particle D_{eq,SA} (μm)</i>	<i>T_{ign delay} (ms)</i>
2400	1	865.3	4.21
	2	643.9	-
	3	725.7	8.21
	4	711.9	-
	5	610.1	4.01
	6	565.3	3.41
	7	796.9	6.91
	8	595.4	4.81
	9	559.1	4.91
	10	826.5	5.11
5500	1	507.6	2.21
	2	806.8	1.91
	3	621.0	1.31
	4	840.5	1.11
	5	861.1	2.11
	6	306.2	0.72
	7	1115.5	1.01
	8	971.9	1.31
	9	825.8	0.81
	10	954.7	0.81
	11	1073.9	0.71
7700	1	728.5	0.28
	2	811.9	0.51
	3	753.0	0.44
	4	664.6	0.39
	5	771.5	0.11
	6	559.0	0.19
	7	871.4	0.08
	8	498.7	0.34
	9	828.9	0.16
	10	893.3	0.09
	11	711.2	0.25